Orbital ordering in Ca_2RuO_4 investigated by ^{99}Ru perturbed angular correlation

M. Rams, M. Krużel, A. Zarzycki, K. Królas, and K. Tomala
M. Smoluchowski Institute of Physics, Jagiellonian University, Reymonta 4, 30-059 Kraków, Poland
(Received 27 November 2008; revised manuscript received 22 June 2009; published 23 July 2009)

The γ-γ perturbed angular correlation technique (PAC) using ^{99}Ru was applied to investigate the orbital ordering of Ru 4*d* electrons in Ca_2RuO_4. It was confirmed that the ferro-orbital ordering characterized by the double occupation of d_{xy} orbitals at every Ru ion is realized in the stoichiometric Ca_2RuO_4. A strong temperature dependence of the quadrupole interaction below the metal-insulator transition around 360 K reflects variation in the occupation of crystal field orbitals enhanced by very pronounced change in the lattice parameters. Temperature dependence of the hyperfine magnetic field H_{hf} at the Ru site shows very steep increase just below the ordering temperature, which could suggest a two-dimensional character of the magnetic ordering in Ca_2RuO_4.

DOI: 10.1103/PhysRevB.80.045119 PACS number(s): 71.30.+h, 76.80.+y

I. INTRODUCTION

The discovery of unconventional superconductivity in Sr_2RuO_4 (Ref. 1) caused a growing interest in the investigation of ruthenium oxides of the Ruddlesden-Popper series $(Ca,Sr)_{n+1}Ru_nO_{3n+1}$. Their crystal structures contain RuO_2 layers built up of corner sharing RuO_6 octahedra. For $n=1$, Sr_2RuO_4 has the tetragonal structure with the $I4/mmm$ space group. The smaller size of Ca^{2+} ions in Ca_2RuO_4 leads at low temperatures to the orthorhombic structure described by the space group *Pbca*.[2,3] The orthorhombic distortion of the crystal structure results in totally different physical properties of Ca_2RuO_4 in comparison with its strontium analog. Instead of the two-dimensional Fermi liquid behavior observed in the metallic Sr_2RuO_4, the deformation of O–Ru–O chains (the O–Ru–O angle amounts to only 151° instead of 180° as it is in the tetragonal Sr_2RuO_4) leads in Ca_2RuO_4 to the considerable decrease in the 4*d* bandwidth and in consequence to the Mott insulating ground state with an antiferromagnetic order at low temperatures.

A lot of attention was devoted to theoretical and experimental investigations of the Ca_2RuO_4 electronic structure, where Ru^{4+} ions contain four 4*d* electrons distributed within the t_{2g} energy levels in the low-spin configuration with $S=1$. Because of the compression of RuO_6 octahedra along the *c* axis, the t_{2g} state is split by the crystal electric field (CEF) of essentially tetragonal symmetry into the ground d_{xy} and excited d_{yz}/d_{zx} orbitals.[3] In this situation, it would be expected that two 4*d* electrons of opposite spins occupy the ground d_{xy} level (zero holes in the d_{xy} orbital) and two remaining electrons are located in d_{yz}/d_{zx} (two holes in the d_{yz}/d_{zx} orbitals). This occupation, which leads to exactly the same distribution of 4*d* electrons at every ruthenium site is defined as the state with a ferro-orbital (FO) ordering and was predicted by theoretical calculations.[4,5] However, different conclusions concerning the electronic structure of ruthenium ions were drawn from O 1*s* x-ray absorption spectra, which are sensitive to the occupation of individual d_{ij} orbitals $(ij=xy,yz,zx)$.[6] The authors estimated the number of 0.5 holes (1.5 electrons) in the d_{xy} orbital and 1.5 holes (2.5 electrons) in the d_{yz}/d_{zx} orbitals, in distinct disagreement with expectations.[6] This result was immediately explained by theoretical calculations presented in Ref. 7, where the antiferro-orbital (AFO) ordering characterized by a different occupation of d_{ij} orbitals in adjacent Ru atoms was postulated [see Fig. 1(d) in Ref. 7]. The proposed AFO ordered state leads to the distribution of holes within d_{xy} and d_{yz}/d_{zx} orbitals, with occupations being in agreement with experimental results.[6] The next experiment suggested coexistence of both FO and AFO orderings.[8] Nevertheless, following papers devoted to this problem support the presence of the FO ordering. First of all, results of optical investigations, supplemented by band structure calculations using the LDA+U method, show the d_{xy} FO ordering in the ground state.[9] In addition, very strong variation in the electronic structure (the hole population among different orbitals) with increasing temperature was detected. Then, the presence of the same kind of FO ordering was inferred from resonance X-ray interference measurements.[10,11]

In this paper, the possible orbital ordering of the ruthenium 4*d* electrons in Ca_2RuO_4 was explored by investigation of the quadrupole interaction between valence electrons of Ru ions and the electric quadrupole moment of the ruthenium nucleus. The valence part of the electric field gradient (EFG) tensor produced at the Ru nucleus by t_{2g} electrons depends on the occupation of the t_{2g} orbitals. As it will be explained in detail, the orbital ordering connected with different occupations of d_{xy}, d_{yz}, and d_{zx} orbitals at adjacent Ru ions should lead to different EFG. To measure the quadrupole interaction energy, the technique of perturbed angular correlation with ^{99}Ru isotope was employed. The final conclusions concerning the charge distribution of 4*d* electrons in Ca_2RuO_4, being in agreement with the results reported in Refs. 9–11, demonstrate the utility of this method in investigation of the orbital ordering in solids.

The paper has been organized in the following way. In the next section, the experimental details concerning preparation of the sample as well as results of the x-ray diffraction and bulk magnetic measurements used to characterize our Ca_2RuO_4 material are given. That section contains also a short description of the PAC technique and gives indispensable information necessary to understand the experimental results. A presentation of experimental PAC spectra and a description of their analysis are placed in Sec. III. Finally,

Sec. IV contains the discussion of inferred results. At the end of the paper, a short summary of results and some final conclusions are given.

A. *S* and *L* phases and magnetic structure of Ca_2RuO_4

Two different phases of Ca_2RuO_4 that differ in the oxygen content were discovered when the compound was synthesized as a polycrystalline material by the solid state reaction.[2,3] The most accurate structural investigations show that both phases are described by the same orthorhombic space group. They differ mostly in the length of the *c* axis that amounts to $c \simeq 11.94$ Å in the stoichiometric *S* phase and $c \simeq 12.35$ Å in the oxygen excess *L* phase (which is called O-Ca_2RuO_4 in Ref. 3).

The *S* and *L* phases show slightly different magnetic behavior. The *L*-phase crystal orders below $\simeq 160$ K and shows a small ferromagnetic component in the ordered state. The magnetic susceptibility of the *S*-phase material shows the transition to an antiferromagnetic state at $T_N = 110$ K with some additional magnetization below 160 K, which shows the features characteristic for the *L*-phase sample. This was interpreted as caused by possible small inclusions of the "ferromagnetic" *L* phase into the polycrystalline *S*-phase material.[2]

Bulk magnetic properties of both phases were elucidated by the determination of their magnetic structures by neutron diffraction.[3] It was found that both of them show essentially the same antiferromagnetic arrangement of Ru magnetic moments, which are parallel to the orthorhombic *b* axis. The rotation of RuO_6 octahedra around the *c* axis induces a small ferromagnetic component by the Dzyaloshinski-Moriya exchange mechanism. These ferromagnetic components are parallel in adjacent RuO_2 planes in the *L* phase [the magnetic structure shows the *B*-centered magnetic mode with the (0,1,0) propagation vector] leading to the small bulk ferromagnetic moment, whereas they cancel in adjacent planes in the *S* phase [the *A*-centered mode with the (1,0,0) propagation vector].[3] It seems that the neutron diffraction results, giving magnetic transitions in a very good agreement with the bulk magnetic measurements, confirm the existence of inclusions of the *L*-phase material in the *S* phase by detection of the admixture of the *B*-centered mode in the magnetic diffraction spectrum of the *S*-phase material. Finally, one should mention that observed inclusions of the *L* phase into the stoichiometric *S*-phase material are probably a result of the polycrystalline synthesis since the magnetic susceptibility of Ca_2RuO_4 single crystals shows only the antiferromagnetic maximum at 110 K, without any ferromagnetic contribution around 160 K.[9,12]

II. EXPERIMENTAL DETAILS

A. Sample preparation and characterization

The polycrystalline sample of Ca_2RuO_4 was prepared by a standard solid state reaction from RuO_2 and $CaCO_3$. The powders were weighted in a proper molar ratio, mixed in the agate mortar, pressed into a pellet and prereacted at 800 °C for several hours. Following the prescription given in Ref. 2, the final reaction was performed in flowing 99%Ar+1%O_2 gas slightly above 1360 °C, the temperature necessary to obtain the *S*-phase material.

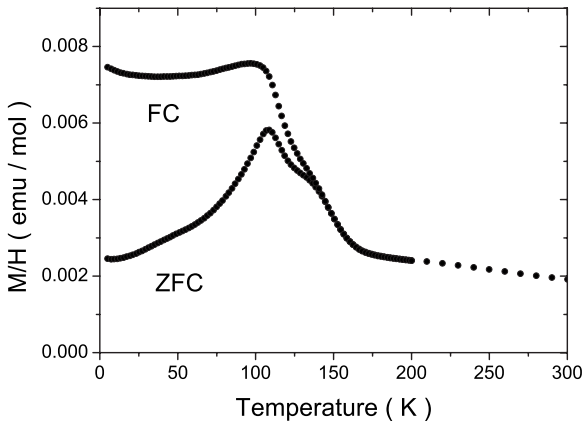

FIG. 1. Zero-field-cooled and field-cooled susceptibility measured in Ca_2RuO_4 at H=10 kOe.

The x-ray diffraction spectrum was measured with Siemens D501 powder diffractometer using Cu K_α radiation and the analysis was performed using the Rietveld method. The spectrum, very similar to the one identified as the *S*-phase,[2] was successfully described within the orthorhombic *Pbca* space group with the lattice constants being in very good agreement with data presented in Ref. 2.

The bulk magnetic properties were examined using a SQUID magnetometer (Quantum Design MPMS-XL5). Zero-field-cooled (ZFC) and field-cooled (FC) measurements of the temperature dependence of the magnetic susceptibility were performed in the external field of $H=10$ kOe, always with increasing temperature (see Fig. 1). The distinct maximum observed at $T_N \simeq 110$ K in FC magnetization corresponds to the antiferromagnetic ordering of the stoichiometric *S*-phase material. Additional magnetization which appears below approximately 160 K has the ferromagnetic character as can be seen from a large difference between FC and ZFC susceptibilities. Following the already mentioned conclusions presented in Refs. 2 and 3, we interpret this as caused by inclusions of the *L*-phase material into the essentially *S*-phase sample.

B. PAC with ^{99}Ru isotope

The measurements of γ-γ perturbed angular correlation (PAC) were performed using $^{99}Rh \rightarrow {}^{99}Ru$ decay ($T_{1/2}=16$ d). The required ^{99}Rh was produced directly in the Ca_2RuO_4 sample, containing the natural abundance of ^{99}Ru, by the $^{99}Ru(p,n)^{99}Rh$ reaction with 30 MeV protons in the cyclotron of the Institute of Nuclear Physics in Kraków. Following the irradiation, the sample was annealed to remove radiation defects, and left for one week for short living isotopes to decay.

Two γ-γ cascades: 528–89 keV and 353–89 keV, as shown in Fig. 2, (with theoretical anisotropy $A_2=-15\%$ and -19%, respectively), were used. The first cascade allows to avoid the background of the 307 keV line of $^{101}Rh(T_{1/2}=4.4$ d), but after several weeks the second cascade gives

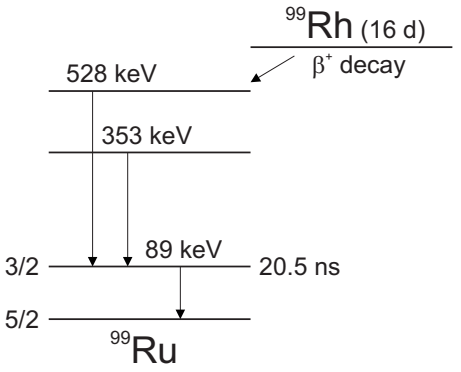

FIG. 2. Partial decay scheme of $^{99}Rh \rightarrow {}^{99}Ru$ with transitions used in PAC measurements.

better signal to noise ratio. The intermediate level of both cascades has spin $I=3/2$ and $T_{1/2}=20.5$ ns.

The measurement setup with four counters with BaF_2 scintillator crystals was used to detect γ radiation. Two of them were 50 mm thick to ensure enough efficiency for high-energy photons, two remaining for counting 89 keV photons were 3 mm thick to reduce the background signal. It took from 1 to 3 days to collect data for each individual PAC spectrum.

C. Analysis of PAC spectra

The PAC spectra were analyzed using combined magnetic and quadrupole hyperfine interaction Hamiltonian $\hat{H}$, which for a nuclear state of spin I, written in the system of principal axes of the EFG tensor, has the form[13]

$$\hat{H} = -g_N\mu_N H_{\rm hf}\left[\hat{I}_z\cos\theta + \frac{1}{2}(\hat{I}_+e^{-i\phi} + \hat{I}_-e^{i\phi})\sin\theta\right] + \frac{eQV_{zz}}{4I(2I-1)}\left[3\hat{I}_z^2 - I(I+1) + \frac{\eta}{2}(\hat{I}_+^2 + \hat{I}_-^2)\right]. \quad (1)$$

In the above equation $H_{\rm hf}$ is the value of the hyperfine magnetic field, V_{zz} denotes the principal component of the diagonalized EFG tensor, and $\eta=(V_{xx}-V_{yy})/V_{zz}$ is the EFG asymmetry parameter. The angles θ and ϕ describe the direction of $\vec{H}_{\rm hf}$ with respect to the EFG principal axes system, θ being the angle between the z axis and $\vec{H}_{\rm hf}$. The $\hat{H}$ was diagonalized numerically and the theoretical perturbation factor $R(t)=A_2^{\rm eff}G_{22}(t)$ was calculated using the general formula for $G_{22}(t)$ function for polycrystalline samples.[13,14] If $H_{\rm hf}=0$, i.e., for pure quadrupole interaction, the $R(t)$ for $I=3/2$ reduces to simpler form

$$R(t) = A_2^{\rm eff}\left[\frac{1}{5} + \frac{4}{5}\cos\left(\frac{\omega_Q t}{2}\sqrt{1+\eta^2/3}\right)\right]. \quad (2)$$

The values of $\omega_L=|g_N\mu_N H_{\rm hf}/\hbar|$, and $\omega_Q=|eQV_{zz}/\hbar|$ were fitted and are used in this paper. The $H_{\rm hf}$ and V_{zz} values can be calculated using factors $Ig_N=-0.284(6)$ and $Q=0.23(1)$ b for the 89 keV level of ^{99}Ru.[15]

There are several restrictions concerning the hyperfine parameters, which can be derived from PAC spectra. First, only the absolute values of V_{zz} and $H_{\rm hf}$ can be determined using γ-γ PAC. Then, for $\eta=0$ the $R(t)$ function does not depend on the ϕ angle. Finally, if $H_{\rm hf}=0$ and $I=3/2$, then ω_Q and η cannot be determined independently, only the product $\omega_Q\sqrt{1+\eta^2/3}$ can be obtained.

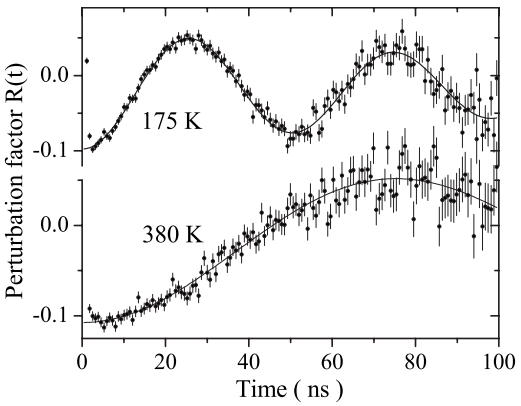

FIG. 3. PAC spectra measured with ^{99}Ru in Ca_2RuO_4 in the paramagnetic region. The solid lines represent the least-squares fit to the experimental points assuming two contributions of pure quadrupole interaction.

III. EXPERIMENTAL RESULTS

The PAC measurements with Ca_2RuO_4 were performed from 23 to 520 K. Two spectra measured at high temperatures are shown in Fig. 3, and sample spectra collected in the magnetic phase are shown in Fig. 4.

To describe consistently all the spectra it was necessary to assume that two components with different hyperfine parameters are present. The major component (denoted here as S) has the weighting factor of 0.70(3), the second component L has remaining 0.30(3) fraction. The correspondence between

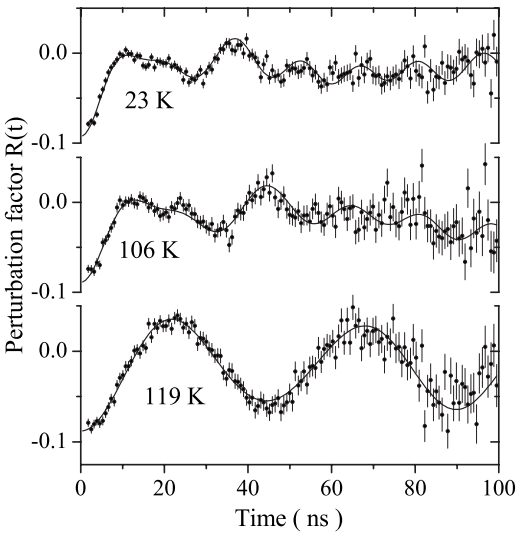

FIG. 4. PAC spectra measured with ^{99}Ru in Ca_2RuO_4 below and just above T_N. The solid lines are fits with the perturbation function for the combined quadrupole and magnetic-hyperfine interactions.

TABLE I. Hyperfine interaction parameters of ^{99}Ru in Ca_2RuO_4.

T(K)	Component	Fraction	ω_Q(Mrad/s) [a]	η	ω_L(Mrad/s) [b]	H_{hf}(kOe)	θ(deg)
23	S	0.70[c]	295(5)	0.05(0.1)	163(1)	180(4)	82(10)
175	S	0.70(3)	252(3)	0[c]			
520	S	0.70[c]	84(8)	0[c]			
23	L	0.30[c]	216(20)	0[c]	134(10)	148(11)	45[c]
175	L	0.30(3)	184(10)	0[c]			
520	L	0.30[c]	52(12)	0[c]			

[a] $\omega_Q = |eQV_{zz}/\hbar|$.
[b] $\omega_L = |g_N \mu_N H_{hf}/\hbar|$.
[c] Parameter fixed during analysis.

$L(S)$ components, and $L(S)$ phases will be justified in the next section.

The spectra at low temperatures are rich in features, which allow us to determine precisely ω_L and ω_Q for the majority component. Besides, θ can be determined as close to 90° and η as close to zero. The obtained hyperfine parameters of selected spectra are gathered in Table I. During analysis of the spectra taken above 78 K, η was fixed as 0.0, and θ as 90°. Finally, close to the magnetic transition temperature $T_N \simeq 110$ K only ω_L of the majority component was allowed to vary. The obtained temperature dependence of H_{hf} calculated from ω_L is presented in Fig. 5 with solid dots. At higher temperatures only the pure quadrupole interaction $R(t)$ is expected, so ω_L was fixed as zero, and only ω_Q was fitted. The temperature dependence of ω_Q is shown in Fig. 6.

The hyperfine parameters cannot be determined so precisely for the minority component L. To reduce the number of free parameters we assumed θ=45° and η=0 in this case (for arguments see the next section). This component shows a magnetic transition at 150(10) K and the temperature dependence of H_{hf} and quadrupole interaction are marked with open symbols in Figs. 5 and 6, respectively.

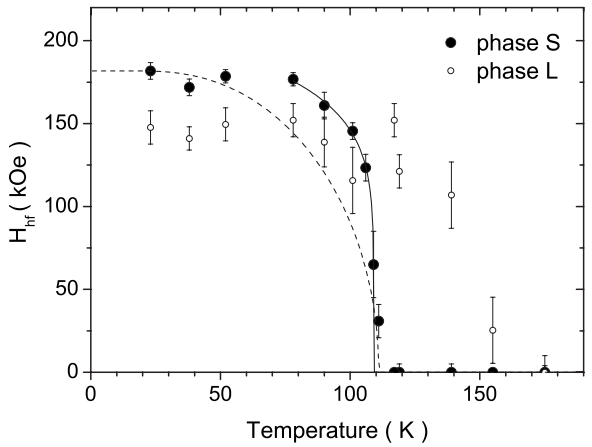

FIG. 5. Temperature dependence of the magnetic-hyperfine field at the Ru site for two magnetic phases in Ca_2RuO_4. The dotted line represent the magnetization calculated in the mean-field approximation with S=1; the solid line is and the fitted critical exponent dependence (see text).

IV. DISCUSSION

The aim of this paper is to discuss a possible orbital ordering of the 4*d* Ru electric charges, more precisely, to distinguish between two theoretically justified types of orbital ordering: FO and AFO. In the case of the Ru^{4+} ion with four 4*d* electrons in the low-spin state, three electrons occupy d_{xy}, d_{yz}, and d_{zx} CEF levels with the same spin direction (Hund's rule), which gives spherically symmetric 4*d* electron charge distribution. The orbital ordering is determined by the fourth electron with the opposite spin direction, which has to occupy one of d_{ij} levels, and leads to the charge distribution asymmetry.

The orbital patterns for FO and AFO orderings are shown in Fig. 7 as the charge distribution of the 4*d* electrons localized at four adjacent Ru sites in the RuO_2 plane. These patterns can be translated to the double occupation of the t_{2g} sublevels by the fourth electron. In the FO ordering all Ru ions show the double occupation of d_{xy} levels, giving the occupation of zero and two holes in the d_{xy} and d_{yz}/d_{zx} orbitals, respectively. In case of the AFO ordering at some Ru sites the d_{yz} or d_{zx} orbitals are double occupied, which leads to the average occupation 0.5 holes in d_{xy} and 1.5 holes in d_{yz}/d_{zx} orbitals.

At the next step, the relationship between experimentally determined quadrupole interaction energy and the electronic structure of ruthenium ions, as well as the relationship be-

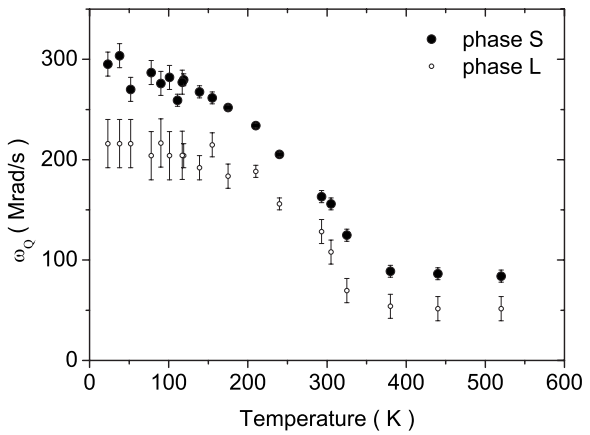

FIG. 6. Temperature dependence of the quadrupole interaction frequency for two components in ^{99}Ru PAC spectra in Ca_2RuO_4.

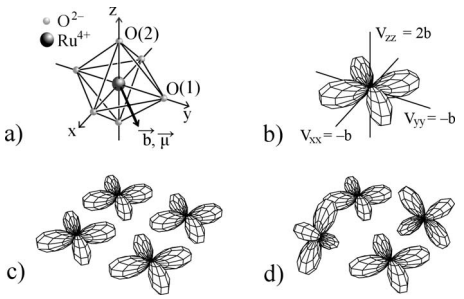

FIG. 7. (a) The octahedral coordination of Ru by O^{2-} ions in Ca_2RuO_4. Despite the global orthorhombic symmetry, at low temperatures the octahedron is only compressed along the z axis and the local symmetry of the Ru-site is almost tetragonal: d[Ru-O(2)]=1.972(2) Å, d[Ru-O(1)]=2.018(2) Å and d[Ru-O(1)]=2.015(2) Å at 11 K.[3] O(2) and O(1) denote the apical and in-plane oxygen ions. (b) Charge distribution within the d_{xy} orbital with EFG V_{ii}^{val} components. (c) Orbital pattern for FO ordering. (d) Orbital pattern for AFO ordering.

tween the possible orbital ordering of ruthenium electrons in Ca_2RuO_4 and the form of the expected PAC spectra have to be considered.

The hyperfine interaction Hamiltonian (1) contains, related to the distribution of electron charges, EFG specified by two parameters: V_{zz} and η. As a rule, the choice of the z axis in the system of principal axes is done following the convention $|V_{zz}| \geq |V_{xx}| \geq |V_{yy}|$. In general, in insulating materials there are two contributions to EFG: the lattice contribution V_{ii}^{lat} caused by electric charges of surrounding ions and the valence contribution V_{ii}^{val} caused by the charge distribution of valence electrons. Both contributions disappear in the case of a cubic symmetry.

In Ca_2RuO_4 at low temperatures the nearest surrounding of Ru ions is comprised of six O^{2-} ions arranged in a slightly distorted, compressed along the z-axis octahedron [see Fig. 7(a)]. For this reason, a nonzero V_{ii}^{lat} contribution is expected. The system of principal axes of V_{ii}^{lat} agrees with the (x,y,z) system shown in the Fig. 7(a), with the principal $V_{zz}^{\mathrm{lat}}=2a$ component parallel to the z axis. In addition, $V_{xx}^{\mathrm{lat}}=V_{yy}^{\mathrm{lat}}=-a$.

As far as the valence contribution to the EFG is concerned, it disappears when all d_{xy}, d_{yz}, and d_{zx} orbitals are occupied by the same number of electrons. Therefore, for the Ru^{4+} ion in the low-spin state, only the location of the fourth electron determines the valence contribution. In the case of doubly occupied d_{xy} orbital

$$V_{zz}^{\mathrm{val}}(d_{xy}) = \frac{4}{7}e(1-R)\langle r^{-3}\rangle_{4d} = 2b \tag{3}$$

and

$$V_{xx}^{\mathrm{val}}(d_{xy}) = V_{yy}^{\mathrm{val}}(d_{xy}) = -b, \tag{4}$$

where estimated $\langle r^{-3}\rangle_{4d} \simeq 4.2$ a.u. (Ref. 16) and the Sternheimer factor $R=-0.06$.[17] The total principal component of EFG, denoted as $V_{z'z'}$ in the following, amounts to $V_{z'z'}(d_{xy})=2a+2b$. An additional piece of information is available when the magnetic hyperfine field is present. Because usually the direction of H_{hf} is close or parallel to the direction of the ruthenium magnetic moment, which in Ca_2RuO_4 is placed in the basal plane, parallel to the orthorhombic b axis [Fig. 7(a)],[3] for doubly occupied d_{xy} orbital the PAC spectrum should be described with H_{hf} directed perpendicular to the $V_{z'z'}$ axis ($\theta \simeq 90°$).

In the case of the double occupation of either d_{yz} or d_{zx} orbitals, the principal component of the valence EFG should have the same magnitude as in the previous (d_{xy}) case but in the direction of x or y axes. The direction of the total $V_{z'z'}$ depends in this case on relative magnitudes of the lattice and the valence contributions. For much smaller lattice part in comparison with the valence contribution $V_{z'z'}=-a+2b$ and points in x or y directions, so PAC spectra should be described by $\theta \simeq 45°$. All above considerations are summarized in Table II.

To justify the dominant valence contribution at low temperatures in Ca_2RuO_4 we have roughly estimated the a value from the point charge model (pcm). We got $\omega_Q^{\mathrm{lat}}=(2a)eQ/\hbar = -125$ Mrad/s taking the crystal structure of Ca_2RuO_4 at 11 K.[3] To take into account the proper value of the Sternheimer factor γ_∞, the deformation of neighbor ions from point charges, and uncertainty of Q, pcm calculations were performed also for other compounds built of RuO_6 octahedra. Then the common scaling factor $Q(1-\gamma_\infty)=3.0$ b was adopted to achieve agreement in the following cases. In $RuSr_2GdCu_2O_8$, where the experimentally determined by NMR $\omega_Q=+51$ Mrad/s (Ref. 18) can be treated as the lattice contribution (Ru^{5+}, $3d^3$ state), the calculated value is +48 Mrad/s. The second test is Ca_2RuO_4 itself, but in the

TABLE II. Enumeration of possible EFGs for various kinds of orbital ordering in Ca_2RuO_4. The lattice gradient $V_{zz}^{\mathrm{lat}}=2a$ is directed along the z axis. The valence gradient $V_{zz}^{\mathrm{val}}=2b$ for d_{xy} orbital, but is rotated for d_{zx} and d_{yz} states.

Ordering	State	V_{xx}	V_{yy}	V_{zz}	$V_{z'z'}$ [a]	θ [b]
FO	$4\times d_{xy}$	$-a-b$	$-a-b$	$2a+2b$	$2a+2b$	90°
AFO	$2\times d_{xy}$	$-a-b$	$-a-b$	$2a+2b$	$2a+2b$	90°
	$1\times d_{yz}$	$-a+2b$	$-a-b$	$2a-b$	$-a+2b$	≃45°
	$1\times d_{zx}$	$-a-b$	$-a+2b$	$2a-b$	$-a+2b$	≃45°

[a] $V_{z'z'}$ is the principal component of V_{ii} and corresponds to V_{zz} in the Hamiltonian (1). The choice here is made assuming the dominant valence contribution.

[b] θ is the angle between the $\vec{b}$ axis on Fig. 7(a) and $V_{z'z'}$ direction. Taking into account the magnetic structure, it corresponds to the θ angle in the Hamiltonian (1). Detailed discussion of the θ angle is given in the text.

metallic phase above 400 K, where V_{ii}^{val} is negligible due to broadening and overlapping of d_{ij} levels, and due to the temperature factor. The experimental value +85 Mrad/s agrees with the calculated +84 Mrad/s.

The valence contribution $\omega_Q^{\mathrm{val}}=(2b)eQ/\hbar=+860$ Mrad/s estimated using Eq. (3) is significantly bigger than ω_Q^{lat}. Experimental data from Table. I together with ω_Q^{lat} gives $\omega_Q^{\mathrm{val}} \simeq +400$ Mrad/s. An exact calculation of EFG would require the accurate *ab initio* calculations,[19,20] which would take into account also the broadening and overlapping of d_{ij} levels. The last effect leads to reduction of the valence contribution.

We can finally postulate the following relationship between the possible orbital orderings in Ca_2RuO_4 and the experimental PAC spectra. In the case of the FO ordering, where all Ru ions have doubly occupied d_{xy} orbitals [Fig. 7(c)], only a single component with unique H_{hf} and $V_{z'z'}$, and with $\theta=90°$ is expected in the spectrum. In the case of the AFO ordering [Fig. 7(d)], one should observe two components: the first characteristic for the situation with doubly occupied d_{xy} orbital described above, and the second with rather different $|V_{z'z'}|$ (presumably also with different H_{hf}) and $\theta \simeq 45°$. It is important to notice that both components should have exactly the same intensities.

The interpretation of our experimental results is complicated by the fact that Ca_2RuO_4 sample used in our investigations is not pure and contains some inclusions of the oxygen excess *L* phase in the stoichiometric *S*-phase material. Since the *L*-phase has different lattice parameters and even the oxygen octahedron has different shape being rather compressed along one of the Ru–O(1) bonds in the basal plane[3] one can expect that PAC spectra for both phases are different. Therefore, even in the case of the FO ordering, we expect at least two components in the PAC spectra with intensities reflecting the amount of the *L*-phase inclusions in the stoichiometric Ca_2RuO_4.

The experimental PAC spectra can be very well reproduced with two components which show different magnitudes of the hyperfine parameters and different relative intensities. Two components were ascribed to two different phases present in our Ca_2RuO_4 sample and some justifying arguments are given below. In our opinion, the majority component with approximately 70% intensity should be ascribed to the stoichiometric *S* phase Ca_2RuO_4. The most important argument comes from the temperature dependence of H_{hf}, which decreases to zero at $\simeq 110$ K, it means at T_N of the stoichiometric compound (Fig. 5). This behavior of H_{hf} can be directly observed in Fig. 4 by the comparison of the PAC spectrum at 106 K which still shows the magnetic perturbation with the completely different spectrum obtained at 119 K where the majority component shows only the quadrupole interaction. The minority component with 30% intensity is caused by the *L*-phase inclusions since PAC spectra between 110 and 150 K are much better reproduced when the magnetic-hyperfine interaction is included in the analysis for this component, in agreement with the results of the bulk magnetic measurements. Because of the low intensity, the inferred hyperfine parameters are not so well established which is reflected by large error bars in Figs. 5 and 6. Since the RuO_6 octahedron in the *L*-phase compound even at low temperatures is compressed along one of Ru-O(1) bonds in the basal plane,[3] which should direct $V_{z'z'}$ along either *x* or *y* axes, the spectra with magnetic perturbations for the *L* component were analyzed with constrained $\theta=45°$.

From the above considerations we can conclude that for the pure and stoichiometric Ca_2RuO_4 there is only the single component in the PAC spectra in the whole range of temperatures. At low temperatures where H_{hf} is present, the analysis shows that $\theta \simeq 90°$, which points to the double occupation of d_{xy} orbitals for each Ru ion. Therefore our PAC measurements demonstrate that in Ca_2RuO_4 the d_{xy} FO ordering is realized, in agreement with Refs. 9–11.

Figure 6 shows a very strong temperature dependence of the quadrupole interaction below the insulator-metal transition (MIT) around $T_{\mathrm{MIT}} \simeq 360$ K.[5,12] In transition metal compounds such behavior is mostly caused by the temperature variation in the occupation of CEF levels (in our case d_{xy}, d_{yz}, and d_{zx} orbitals), since the lattice part of the EFG tensor is almost temperature independent. The Boltzmann statistics leads to the decrease in V_{zz}^{val} with increasing temperature, which is really observed experimentally. Usually such mechanism allows to perform a quantitative analysis of this temperature dependence with adjusted energies of CEF levels and the constant lattice contribution. However, in Ca_2RuO_4 the situation seems to be more complicated. There is a very strong variation in lattice constants with temperature in the insulating phase, including the drastic changes in the octahedral surrounding of Ru-ions (see Fig. 2 in Ref. 21 where results of very detailed structural investigations are presented). Therefore, the assumptions about the temperature-independent lattice contribution and energies of CEF levels are not fulfilled.

The characteristic feature of the temperature dependence of the quadrupole interaction in the insulating phase is the smooth decrease in ω_Q until the MIT is achieved. In particular, one cannot detect any distinct anomaly of ω_Q around 250 K where a possibility of another phase transition was suggested.[10] Either the transition is not accompanied by the variation in the electric charge distribution within the ruthenium 4*d* shell or the changes are so small that they cannot be detected by the observation of the quadrupole interaction. One should also remark that no anomaly of the lattice constants and no abrupt change in the shape of the RuO_6 octahedra have been observed around this temperature.[3,21]

Finally, we observe that the quadrupole interaction is constant above the MIT temperature. This is the consequence of the temperature-independent lattice parameters and lack of the valence contribution above $\simeq 360$ K.

The hyperfine magnetic field saturates at $|H_{\mathrm{hf}}(0)| = 180(10)$ kOe. Since nothing is known about the transferred contribution to the hyperfine field H_{tr} the detailed discussion of the magnitude of the H_{hf} is not possible. Nevertheless, independently of H_{tr} and the sign of H_{hf}, the experimental value is much reduced in comparison with the core polarization contribution H_{core}, which in transition metal compounds usually dominates. For the Ru^{4+} ion this contribution can be estimated taking into account the hyperfine coupling constant $a_{\mathrm{core}} \simeq -300$ kOe/μ_B that gives the core contribution per unpaired spin,[16] and the calculated average spin for the Ru ions in $Ca_2RuO_4 \langle S \rangle \simeq 0.80$ (Ref. 6) (the negative sign of a_{core}

means that the hyperfine field is antiparallel to the ruthenium magnetic moment). Then the core polarization contribution can be estimated as $H_{\text{core}}=2\langle S\rangle\mu_B a_{\text{core}}\simeq -480$ kOe. It seems that the most important source of this reduction is the orbital contribution given by the formula $H_L=2\mu_B\langle r^{-3}\rangle_{4d}\langle L\rangle$. The direction of H_L is parallel to the ruthenium magnetic moment. The average value of the angular momentum for the Ru^{4+} ion in the compressed RuO_6 octahedron was calculated as $\langle L\rangle\simeq 0.68$.[6] The prefactor $2\mu_B\langle r^{-3}\rangle_{4d}$ was estimated as $\simeq 380$ kOe/μ_B, taking into account calculated for Ru^{4+} the value $\langle r^{-3}\rangle_{4d}\simeq 4.2$ a.u., with the reduction factor $\xi=3/4$.[16] Therefore, the orbital contribution to the hyperfine magnetic field can be deduced as equal $H_L\simeq 260$ kOe. Because of the opposite directions of H_{core} and H_L, the second contribution leads to decrease in the total $|H_{\text{hf}}|$. However one should keep in mind that all these calculations are only very rough estimates since the quoted averages $\langle S\rangle$ and $\langle L\rangle$ do not reproduce the value of Ru magnetic moment $\mu(\text{Ru})=1.3\mu_B$ determined by neutron diffraction.[3]

The temperature dependence of the hyperfine-magnetic field (see Fig. 5) confirms the ordering of ruthenium moments in the stoichiometric Ca_2RuO_4 below approximately 110 K. The figure shows also the simulated $H_{\text{hf}}(T)$ calculated within the mean-field approximation for a system with $S=1$, which is very far from the experimental points. A very steep increase in $H_{\text{hf}}(T)$ just below the ordering temperature can be well described using the formula $H_{\text{hf}}(T)\sim(1-T/T_N)^{\beta}$ with parameters $\beta=0.15(8)$ and $T_N=109(1)$ K. The above parameters were obtained from the temperature range of 8% of T_N, but the simulated curve drawn in the Fig. 5 extends to lower temperatures. The estimated value of the critical exponent β, even with the large uncertainty caused by the small number of experimental points, is much closer to 1/8 from the Onsager's solution for the square lattice Ising model, then to $\beta\simeq 5/16$ predicted for a three-dimensional system.[22] This corresponds to the crystal structure of Ca_2RuO_4 that supports strong exchange interactions within the RuO_2 planes and only weak magnetic coupling between distant Ru ions along the c axis.

V. SUMMARY

The paper describes experimental investigations of Ca_2RuO_4 by ^{99}Ru PAC. The essential aim of this work was to gain information about the possible orbital ordering of Ru $4d$ electrons.

The polycrystalline material was prepared by the solid state reaction and characterized by x-ray diffraction and bulk magnetic measurements. It was found that in addition to the stoichiometric S phase the sample contained also inclusions of the unwanted, oxygen excess L-phase material. These inclusions were taken into account during the analysis of the PAC spectra, where they appear as the independent component. The PAC measurements were performed between 23 and 520 K and the hyperfine parameters were determined for the stoichiometric Ca_2RuO_4. The most important conclusion that was deduced concerns the orbital ordering of Ru $4d$ electrons. The extended analysis of the relation between the parameters of PAC spectra and possible orbital orderings, together with the experimental results, point to the conclusion that the d_{xy} ferro-orbital ordering connected with the double occupation of d_{xy} orbitals at every Ru is realized in the stoichiometric Ca_2RuO_4. The strong temperature dependence of the quadrupole interaction frequency ω_Q below the temperature of the metal-insulator transition was qualitatively discussed as being the result of the strong variation in the occupation of d_{ij} crystal field orbitals, additionally enhanced by the pronounced variation in the lattice parameters with temperature. The temperature dependence of the hyperfine magnetic field was determined, with the saturation value of $H_{\text{hf}}(0)=180(10)$ kOe. The very steep increase in H_{hf} directly below the ordering temperature reflects the two-dimensional character of the magnetic ordering in Ca_2RuO_4.

ACKNOWLEDGMENTS

This work was supported by The Polish Ministry of Science and Higher Education, Grant No. 1P03B02429. We also thank the unnamed referees for their useful comments.

[1] Y. Maeno, H. Hashimoto, K. Yosida, S. Nischizaki, T. Fujita, J. G. Bednorz, and F. Lichtenberg, Nature (London) **372**, 532 (1994).
[2] S. Nakatsuji, S. Ikeda, and Y. Maeno, J. Phys. Soc. Jpn. **66**, 1868 (1997).
[3] M. Braden, G. André, S. Nakatsuji, and Y. Maeno, Phys. Rev. B **58**, 847 (1998).
[4] V. I. Anisimov, I. A. Nekrasow, D. E. Kondakov, T. M. Rice, and M. Sigrist, Eur. Phys. J. B **25**, 191 (2002).
[5] Z. Fang, N. Nagaosa, and K. Terakura, Phys. Rev. B **69**, 045116 (2004).
[6] T. Mizokawa, L. H. Tjeng, G. A. Sawatzky, G. Ghiringhelli, O. Tjernberg, N. B. Brookes, H. Fukazawa, S. Nakatsuji, and Y. Maeno, Phys. Rev. Lett. **87**, 077202 (2001).
[7] T. Hotta and E. Dagotto, Phys. Rev. Lett. **88**, 017201 (2001); Physica B **312-313**, 700 (2002).
[8] J. S. Lee, Y. S. Lee, T. W. Noh, S.-J. Oh, Yu. Jaejun, S. Nakatsuji, H. Fukazawa, and Y. Maeno, Phys. Rev. Lett. **89**, 257402 (2002).
[9] J. H. Jung, Z. Fang, J. P. He, Y. Kaneko, Y. Okimoto, and Y. Tokura, Phys. Rev. Lett. **91**, 056403 (2003).
[10] I. Zegkinoglou, J. Strempfer, C. S. Nelson, J. P. Hill, J. Chakhalian, C. Bernhard, J. C. Lang, G. Srajer, H. Fukazawa, S. Nakatsuji, Y. Maeno, and B. Keimer, Phys. Rev. Lett. **95**, 136401 (2005).
[11] M. Kubota, Y. Murakami, M. Mizumaki, H. Ohsumi, N. Ikeda, S. Nakatsuji, H. Fukazawa, and Y. Maeno, Phys. Rev. Lett. **95**, 026401 (2005).
[12] C. S. Alexander, G. Cao, V. Dobrosavljevic, S. McCall, J. E. Crow, E. Lochner, and R. P. Guertin, Phys. Rev. B **60**, R8422 (1999).
[13] H. Frauenfelder and R. M. Steffen, in *Alpha-, Beta-, Gamma-*

Ray Spectroscopy, ch XIXA, edited by K. Siegbahn (North-Holland, Amsterdam, 1968).
[14] T. Butz, Hyperfine Interact. **52**, 189 (1989).
[15] L. K. Peker, Nucl. Data Sheets **73**, 1 (1994).
[16] K. Ishida, Y. Kitaoka, K. Asayama, S. Ikeda, S. Nishizaki, Y. Maeno, K. Yoshida, and T. Fujita, Phys. Rev. B **56**, R505 (1997).
[17] K. D. Sen and P. T. Narasimhan, Phys. Rev. B **16**, 107 (1977).
[18] Y. Tokunaga, H. Kotegawa, K. Ishida, Y. Kitaoka, H. Takagiwa, and J. Akimitsu, Phys. Rev. Lett. **86**, 5767 (2001).
[19] K. Schwarz, P. Blaha, and G. K. H. Madsen, Comput. Phys. Commun. **147**, 71 (2002).
[20] L. A. Errico, G. Fabricius, M. Renteria, P. de la Presa, and M. Forker, Phys. Rev. Lett. **89**, 055503 (2002).
[21] O. Friedt, M. Braden, G. André, P. Adelmann, S. Nakatsuji, and Y. Maeno, Phys. Rev. B **63**, 174432 (2001).
[22] M. E. Fisher, Rev. Mod. Phys. **46**, 597 (1974).